Engineering 61 (2026) 375–388

Contents lists available at ScienceDirect

Engineering

journal homepage: www.elsevier.com/locate/eng

Research
Environmental Frontiers for Water–Energy Nexus—Review

Water Harvesting with Zeolite, MOF, COF, and HOF Adsorbents

Bo Zhang [a,b], Zhi Wang [a,b], Freek Kapteijn [c], Xinlei Liu [a,b,*]

[a] Chemical Engineering Research Center, School of Chemical Engineering and Technology, Tianjin University, Tianjin 300072, China
[b] Tianjin Key Laboratory of Membrane Science and Desalination Technology, State Key Laboratory of Chemical Engineering and Low-Carbon Technology, Tianjin University, Tianjin 300072, China
[c] Catalysis Engineering, Chemical Engineering Department, Delft University of Technology, Delft 2629 HZ, the Netherlands

ARTICLE INFO

Article history:
Received 16 April 2025
Revised 25 September 2025
Accepted 10 October 2025
Available online 23 October 2025

Keywords:
Water adsorption
Water harvesting
Zeolite
Metal–organic frameworks
Covalent organic frameworks
Hydrogen-bonded organic frameworks

ABSTRACT

To deal with global water shortage, water vapor in the air is regarded as a freshwater source that cannot be ignored, especially in water-scarce regions. Adsorption-based atmospheric water harvesting (AAWH) is a promising option that utilizes the interaction between the internal structure of the adsorbent material and water molecules to accumulate water. Novel water harvesting adsorbents such as zeolites, metal–organic frameworks (MOFs), covalent organic frameworks (COFs), and hydrogen-bonded organic frameworks (HOFs) have given new perspectives to fundamentally improve the effectiveness of AAWH, benefiting from their steep S-shaped isotherms. Based on the selection criteria derived from the principle of AAWH, 5 zeolites, 20 MOFs, 6 COFs, and one HOF are identified as potential candidates. From the analysis of the water adsorption mechanisms of these four types of materials and summarizing the latest progress in AAWH devices, the next-generation AAWH technology should focus on the scale-up of well-designed adsorbent components and their integration into efficient system devices to promote the practical application of AAWH.

1. Introduction

Life is inseparable from water, but many areas face severe freshwater shortages. To address this pressing problem, water harvesting and purification technologies have been extensively developed. Among them, atmospheric water harvesting (AWH) stands out as a promising technology with significant recent progress [1]. Technologies like fog and dew collection are not suitable for use in arid regions (relative humidity (RH) less than 30%) because of the high energy consumption needed for condensation under low relative humidity [1–3]. Adsorption-based atmospheric water harvesting (AAWH) is an energy-efficient method that leverages the interaction between the internal structure of the adsorbent and water molecules to accumulate water. Benefiting from the rapid development of adsorbents and devices, AAWH has been demonstrated to be capable of harvesting water in extremely arid regions [4–7].

The working principle of AAWH (Fig. 1(a)) [3] is summarized as follows: The hydrophilic adsorbent adsorbs water molecules from the air into its internal structure to effectively accumulate moisture. Then, using humidity or heat gradients as a driving force, the captured water is released from the adsorbent as rich vapor, which is then condensed into liquid water and collected [3,8,9]. This water harvesting process relies on the ability of the adsorbents to capture and release water vapor through the cyclic adsorption–desorption [10]. Thus, an ideal adsorbent for AAWH should meet the following six criteria [9,11]: ① hydrothermal stability under liquid water and vapor conditions; ② isotherm with a steep uptake at the required relative pressure; ③ reversible water uptake/release at the steep step of isotherm; ④ desorption without hysteresis; ⑤ high and constant water capacity during adsorption–desorption cycling; ⑥ efficient adsorption–desorption with fast heat and mass transport kinetics. Consequently, there are high expectations for the interaction between the adsorbent material and water molecules. The adsorbent needs to have an affinity or strong interaction with water molecules to operate effectively at low relative humidity. In the meantime, the adsorbent–water interaction should be easily interrupted by humidity or heat gradients to release water [12–14]. This interaction is mainly regulated by geometric configuration, pore size, hydrophilicity, and polarity within the adsorbent.

* Corresponding author.
E-mail address: xinlei_liu1@tju.edu.cn (X. Liu).

https://doi.org/10.1016/j.eng.2025.10.011

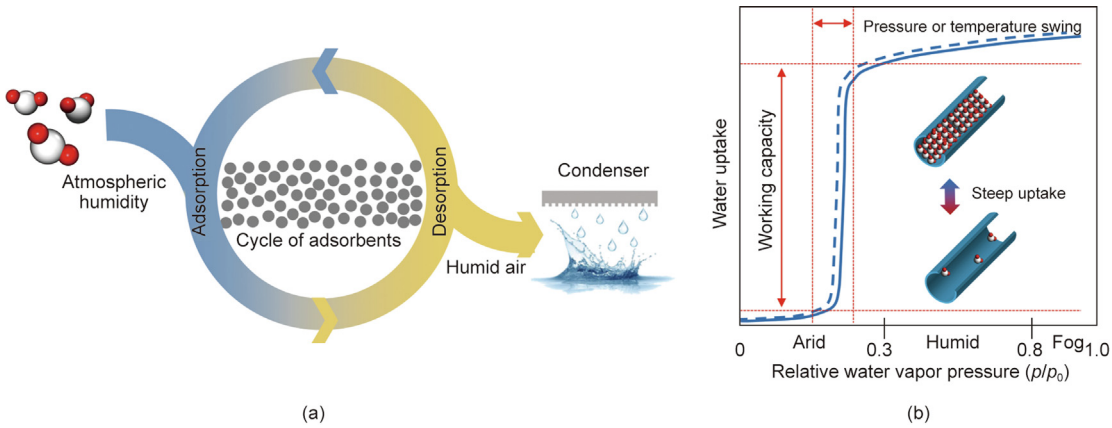

Fig. 1. (a) The working principle of AAWH. Reproduced from Ref. [3] with permission. (b) A characteristic example of stepwise water adsorption (solid line) and desorption (dashed line) isotherms and a scheme of the desired water adsorption–desorption cycle during pressure or temperature swing with the regular ordering of water molecules in an ideal straight pore channel. p represents partial pressure of water vapor. p_0 represents saturated pressure of water vapor. p/p_0 represents relative water vapor pressure.

Precise structural design of adsorbent materials and rational tuning of adsorbent–water interactions are of importance to achieve high water-related performance in both kinetic and thermodynamic properties. In addition to a reasonable distribution of hydrophilic sites [15–18], materials with regular pores also contribute to the formation of unique step-like S-shaped (type V) [19] isotherms [9,11]. Additionally, the regular ordering of adsorbed water molecules, driven by pore size and geometry, results in a nanocrystalline structure [16,20], facilitating the water uptake and release similar to a phase change process [9]. By establishing clear structure–function principles, the simultaneous optimization of thermodynamic and kinetic characteristics of water adsorption and desorption will become a reality, which will improve the utility of adsorbents for AAWH.

A variety of adsorbents have been developed for AAWH. Zeolites, metal–organic frameworks (MOFs), covalent organic frameworks (COFs), and hydrogen-bonded organic frameworks (HOFs), which are crystalline porous materials with ordered and designable structures and adjustable pore environments, followed by S-shaped isotherms (Fig. 1(b)), have received widespread attention. This review in engineering further builds on our previous reviews of MOF-based water adsorption with a focus on arid atmospheric (below 30% RH) water harvesting [9,11], and extends recent literature focusing on the potential of zeolites, MOFs, COFs, and HOFs materials for water harvesting applications. In addition to the highly anticipated MOFs and COFs, which are gaining more new members and a wide range of design strategies, we also emphasize the potential of novel zeolites and HOFs for water adsorption. This paper bridges the innovations in four types of porous materials to device realization from both material and engineering aspects, and also concludes with outlooks on next-generation materials and devices to facilitate practical applications of AAWH.

2. Material aspects

2.1. Zeolites

Zeolites are a category of inorganic porous materials considered suitable for water adsorption applications. With their advantages of low cost and commercial preparation, they are among the earliest porous materials employed in AAWH [21]. As a kind of alumina silicate crystal, the aluminosilicate structure of the zeolite can adsorb water molecules easily. Although zeolites suffer from the drawbacks of low adsorption capacity, high regeneration temperature, and poor thermal conductivity, different grades of zeolites that feature promising properties for AAWH have been introduced [22].

Owing to the presence of $[SiO_4]^{4-}$ and $[AlO_4]^{5-}$ tetrahedra and counterions in the framework, zeolites have a strong adsorption capacity for water molecules and are often used as desiccants [21]. Taking Zeolite Y as an example, due to the strong hydrophilicity of high Al-content zeolites, it features a steep uptake at an extremely low RH. It is recognized that aluminosilicate zeolites, especially those exhibiting a steep uptake at extremely low relative pressure (type I isotherms), typically require excessively high regeneration temperatures. Although the regeneration temperature can be lowered by adjusting the Si/Al ratio [23], the adsorption performance of zeolite will be compromised to a certain extent due to the lower hydrophilicity caused by the lower aluminum content [24]. Therefore, this commonly reported drawback has limited the AAWH application of such zeolites. Fortunately, there is a certain degree of correlation between structural properties of zeolites and their water capacities. The relationship between parameters like framework structure and fractal dimension can serve as an indicator for achieving zeolites with higher water capacity [25]. Analogue zeolite-like materials with varying chemical compositions can be prepared for certain frameworks, potentially offering greater capacity than existing zeolites with the same structure. Even with a limited capacity increase (up to 0.4 $g \cdot g^{-1}$, as shown in Fig. 2(a)), materials with a desirable isotherm shape can still be applied for water harvesting applications.

Several zeolite-like microporous materials, such as aluminophosphates (AlPOs), which feature type V isotherms, might act as effective candidates for AAWH. AlPOs are mainly found as pure AlPOs, ferroaluminophosphates (FAPOs), and silicoaluminophosphates (SAPOs) [26], and most of them feature similar structures to aluminosilicate zeolites. The neutron scattering results indicate that, during the initial adsorption stage, water molecules first occupy the pore walls, subsequently filling the central pore area. The confinement within these channels intensifies water intermolecular interactions, resulting in the formation of ordered hydrogen-bonded water chains [27,28].

Unsubstituted AlPOs: Cage-based AlPO frameworks with neutral frameworks and pore openings exhibit comparable water adsorption capabilities to conventional MOF-303, and regeneration temperatures are below 100 °C [26,29]. EMM-8 (ExxonMobil Material #8) with sodalite framework (SFO topology) features 0.7 nm diameter 12-ring channels, and exhibits a steep step-like uptake at p/p_0 = 0.15 (Fig. 2(a)), a water capacity of 0.39 $g \cdot g^{-1}$, and a low

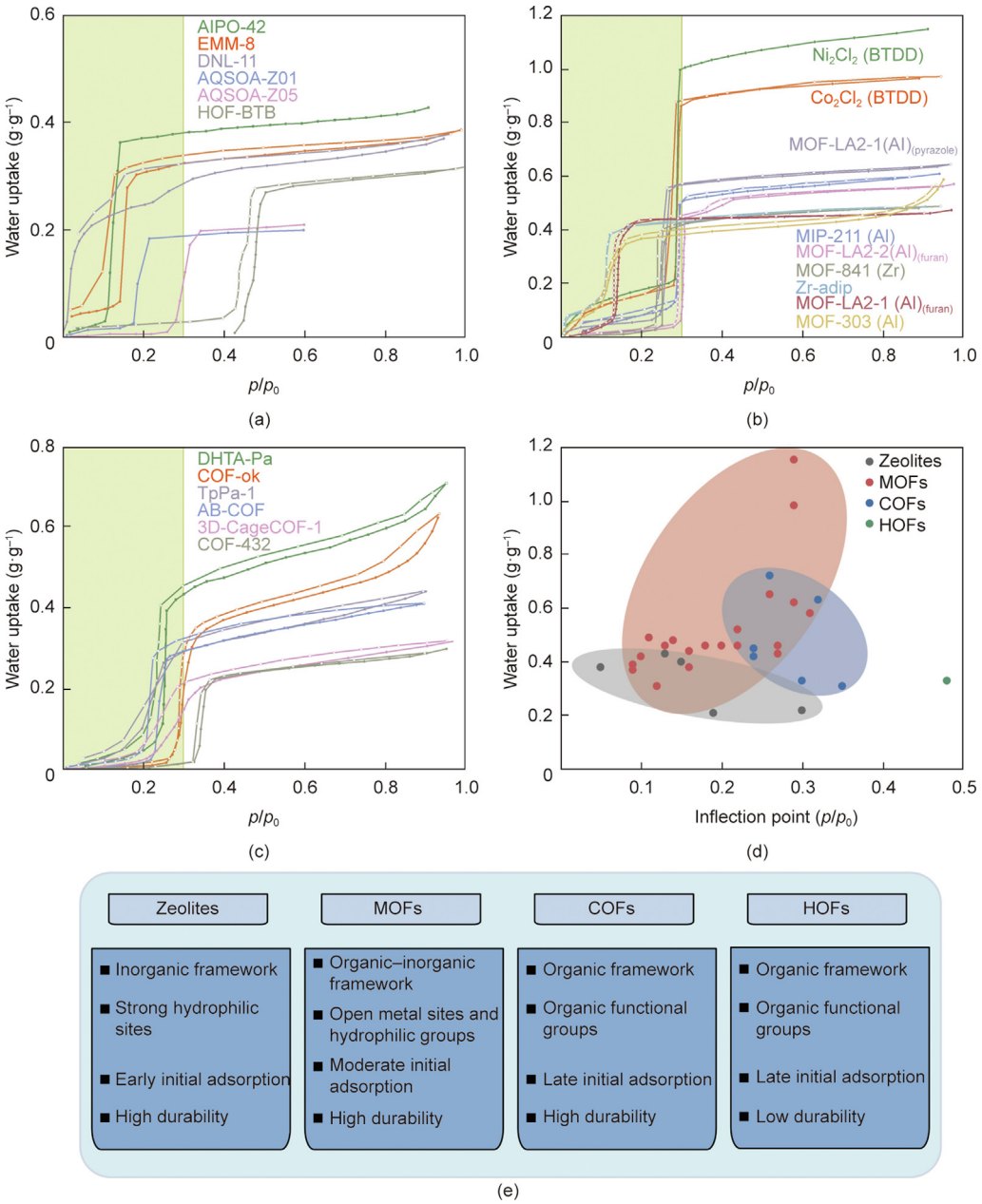

Fig. 2. (a) Water adsorption (solid symbols) and desorption (open symbols) isotherms of the selected zeolites and HOFs. (b) Water adsorption and desorption isotherms of the top nine MOFs with high capacity. (c) Water adsorption and desorption isotherms of the selected COFs. (d) Collected data of zeolites', MOFs', COFs', and HOFs' inflection points at the water adsorption step vs water capacities. (e) Comparison of the chemical composition, adsorption site properties, initial adsorption characteristics and cycling durability of the zeolite, MOFs, COFs, and HOFs. Abbreviations in the figure can be found in Section 2.5.

regeneration temperature of 65 °C. AlPO-Tric has a similar isotherm to EMM-8, but features a higher regeneration temperature of 95 °C [30]. AlPO-42 ($AlPO_4$-LTA), with Linde Type A (LTA) topology [31], shows a steep water uptake at p/p_0 = 0.13 and features the highest water capacity (0.42 $g{\cdot}g^{-1}$) beyond other unsubstituted AlPOs (Fig. 2(a)) [26]. AlPO-42 exhibits moderate adsorption enthalpy and a lower regeneration temperature of 60 °C, thus making it suitable for atmospheric water harvesting [32]. DNL-11 (DNL represents Dalian National Laboratory for Clean Energy, China) with one dimensional (1D) 16-ring channels features a steep uptake at an extremely low relative humidity of p/p_0 = 0.05 (Fig. 2(a)), and most of the adsorbed water can be released via purging with nitrogen at room temperature and ambient pressure, which makes it possible to harvest water in arid areas [29].

SAPOs: Silicon-substituted AlPOs appear to be promising adsorbents in arid environments [5,26]. SAPO-34 with LTA structure, also referred to as FAM-Z02 (FAM-Z represents functional adsorbent material zeolite) or AQSOA-Z02 (AQSOA is a trademark of Mitsubishi Plastics, INC.), features good water adsorption performance. Randomly dispersed Si^{4+} atoms would replace P^{5+}, resulting in extremely acidic Si–OH–Al bridges, which are regarded as water-binding sites and trigger rapid adsorption but also a high adsorption heat [30]. The systematic desorption kinetics study by Hanikel et al. [5] showed that SAPO-34 exhibited inferior desorption kinetics compared to MOF-303(Al) and Al-fumarate, and it can only be completely dehydrated by heating to above 100 °C under test conditions. Therefore, hydrophilic SAPOs may not be suitable for

atmospheric water harvesting devices that pursue energy utilization efficiency.

FAPOs: Although the water capacity of iron-substituted AlPOs is lower than that of SAPOs [26], its suitable regeneration temperature enables its application in practical water harvesting devices (vide infra). FAPO-5, commercially known as FAM-Z01 or AQSOA-Z01, features an AFI type structure in which Al and/or P atoms are partly replaced by Fe heteroatoms [26]. AQSOA-Z01 possesses a type V isotherm with a steep uptake at p/p_0 = 0.19. Although AQSOA-Z01 has a low water capacity of 0.2 $g{\cdot}g^{-1}$ (Fig. 2(a)), its primary advantage is that it can be regenerated at 50–85 °C [33]. FAPO-34 (FAM-Z05 or AQSOA-Z05), without iron substitution, has the same structure as FAPO-5 and exhibits a similar isotherm, but with a higher inflection point at p/p_0 = 0.30 (Fig. 2(a)). This inflection point represents the relative pressure at 50% of maximum capacity.

The properties of the pores in AlPOs provide a framework with highly tunable characteristics. Functionalization using metal substitution involves the insertion of heteroatoms into the framework of AlPOs, either through impregnation, ion exchange, or isomorphous replacement, to alter their hydrophilicity and structural arrangement. The main advantages of AlPOs (Table 1) are their adsorption affinity at low relative humidity (below 20% RH) and S-shaped isotherms, which are suitable for AAWH applications.

2.2. MOFs

With scholars' in-depth understanding of the hydrolysis mechanism of MOFs [12,34], a variety of water-stable MOFs have been born [11], which expands their application scope. Benefiting from their water stability, chemical tunability, crystallinity, and high porosity, MOFs are considered suitable adsorbents for AAWH with reversible binding of water [35]. Through reasonable reticular design [36], an increasing amount of MOFs show attractive water adsorption characteristics and can be utilized as adsorbents for water harvesting from arid air [5]. Based on the six criteria mentioned previously, favorable candidates for AAWH are selected from numerous MOFs (Section 2.5). Based on the differences in design strategies, these MOFs can be primarily divided into the following types, and their structural characteristics and water sorption properties are summarized as follows.

Direct synthesis of MOFs with step-shaped isotherm: Al-fumarate [37] has rigid 1D lozenge-shaped channels (diameter around 0.60 nm) with a steep uptake at p/p_0 = 0.2–0.3 and narrow hysteresis [38]. CAU-23(Al) (CAU represents Christian Albrechts University) [39] features 1D square channels (0.76 nm) and exhibits steep uptake at p/p_0 = 0.27, accompanied by minimal hysteresis. MOF-801(Zr) [40], with face-centered cubic (fcu) topology and three types of pore sizes (0.48, 0.56, and 0.74 nm) [12], shows a steep uptake at p/p_0 = 0.05. The defective Zr-Fum HT (Fum represents fumarate, HT represents hydrothermal synthesis in water solvents) [41] shows a steeper uptake at the inflection point, as well as a larger capacity, compared with the solvothermal synthesized MOF-801(Zr). MOF-841(Zr) [40] has flu topology, 1.33 nm pores, an S-shaped isotherm with a steep uptake at p/p_0 = 0.22, and no hysteresis (Fig. 2(b)). Co-CUK-1 (CUK represents Cambridge University-KRICT) [42] features 1D channels (1.34 nm × 1.3 nm), a type V isotherm with a steep uptake at p/p_0 = 0.12, and no hysteresis. Through rational design of their structures, an increasing number of MOFs with excellent water properties have been synthesized.

SBU modification: By rationally designing and regulating the anions and cations in secondary building units (SBUs), not only can a more water-stable MOF be constructed, but also its inflection point and water capacity can be controlled [36,43]. Cation or anion exchange, the substitution of coordinatively saturated cations with unsaturated cations, which can tune the hydrophilicity of MOFs, has been employed to shift the inflection point [44,45]. For instance, Co_2Cl_2(BTDD) [46] features 1D mesoporous channels (2.2 nm) that slightly shrink to micropores (< 2 nm) after water adsorption, thereby preventing capillary condensation. It shows a steep uptake at p/p_0 = 0.29 (Fig. 2(b)) and a water capacity of 0.97 $g{\cdot}g^{-1}$. Ni_2Cl_2(BTDD), similar to Co_2Cl_2(BTDD), features a larger water capacity of 1.14 $g{\cdot}g^{-1}$ (Fig. 2(b)) [45,47].

Linker modification-functionalised linkers: Modifying MOFs with functionalized linkers featuring hydrophilic or hydrophobic groups can shift the steep uptake step to lower or higher relative humidity [9]. MIP-200(Zr) (MIP represents materials of the Institute of Porous Materials from Paris) [48] features 1D channels (0.68 and 1.3 nm) followed by a type IV isotherm without hysteresis and an inflection point at p/p_0 = 0.18. Zr-adip [49], which incorporates hydrophilic nitrogen sites into MIP-200(Zr), displays a significantly improved uptake in the low range of p/p_0 = 0.1–0.25 (Fig. 2(b)). MIL-125(Ti)-NH_2 (MIL represents Matériel Institut Lavoisier) [50], prepared by decorating NH_2-groups on linkers for a more hydrophilic and robust structure, has a three-dimensional (3D) pore structure (0.6 and 1.2 nm), showing a type V isotherm, a steep uptake at p/p_0 = 0.2, and little hysteresis.

Linker modification-isoreticular expansion: Once the synthetic conditions for forming MOFs with specific SBUs are established, frameworks with the same networks but different pore sizes and environments can be obtained by making minor adjustments to the linkers of the same type but varying in size, length, or side chains [36]. MOF-303(Al) [4] with 1D hydrophilic channels (about 0.6 nm) features a type IV isotherm without hysteresis and an inflection point at p/p_0 = 0.13 (Fig. 2(b)), while the isomorphous MOF-333(Al) with a different linker shows a type V isotherm with steep uptake at p/p_0 = 0.21 [16]. MOF-303(Al) has received attention and application due to its excellent water adsorption performance (vide infra), and its variants have also demonstrated outstanding performance. By adjusting the ratio of $PZDC^{2-}$ (linker of MOF-303(Al)) and FDC^{2-} (linker of MOF-333(Al)), a series of multivariate MOFs exhibits adjustable isotherms in the range of p/p_0 = 0.13–0.21 without affecting water capacity [16]. Also, the linker extension strategy has been widely employed to synthesize new Al-MOFs, achieving a greater water capacity while retaining the advantageous low inflection point of their parent MOF-303(Al). Among them, MOF-LA2-1(Al) (pyrazole) with a longer linker exhibits an approximately 50% increase in water capacity and an increased inflection point from 0.13 to 0.26 (Fig. 2(b)), compared with MOF-303(Al) [17]. By using extended furan-based linkers, MOF-LA2-1(Al) (furan) and MOF-LA2-2(Al) (furan) express steeper isotherms (Fig. 2(b)) with inflection points at p/p_0 = 0.14 and 0.31, respectively, and have higher water capacities than MOF-303(Al) [51]. CAU-10(Al)-H [52] features 1D square-shaped, sinusoidal channels (about 0.7 nm) with an S-shaped isotherm and main loading at p/p_0 = 0.16 without hysteresis [53]. MIL-160(Al) [54], isomorphic to CAU-10(Al) [53], has 1D channels (about 0.5 nm) and features a type V isotherm without hysteresis and a lower inflection point at p/p_0 = 0.09. KMF-1(Al) (KMF represents KRICT-CNRS-Montpellier Framework) [55], isostructural analog of CAU-10(Al), has 1D channels (about 0.57 nm) with an S-shaped isotherm at p/p_0 = 0.16 and no hysteresis. Furthermore, through adjusting the hydrophilicity of MIL-53(Al) by utilizing polymorphism in Al-MOFs, the inflection point of the water isotherm shifts from a p/p_0 of approximately 0.5 for MIL-53(Al)-muc to a p/p_0 of about 0.3 for MIP-211(Al) (Fig. 2(b)) [53].

The hysteresis between the adsorption–desorption branches, due to the thermodynamic irreversibility of capillary condensation, needs to be avoided for AAWH application. As shown in Section 2.5, except for Co_2Cl_2(BTDD) and Ni_2Cl_2(BTDD), in which pore sizes decrease from mesoporous to microporous after water adsorption,

all other MOFs are microporous (<2 nm pore diameter, which is smaller than the critical diameter for water). Hydrophilic microporous MOF follows a reversible pore filling mechanism, where specific adsorption at open metal sites and hydrophilic functional groups initiates nucleation, gradually forming localized water clusters through hydrogen bonding and expanding with increasing relative pressure, ultimately filling the micropores [9,12]. A smaller pore size facilitates the position of the inflection point to move toward a lower relative pressure [9]. To promote water uptake in arid conditions, merely enhancing hydrophilicity would trigger strong binding and the formation of water superclusters, which may cause undesirable hysteresis and difficulty in desorption. On the contrary, water uptake without hysteresis under extremely low relative humidity conditions can be better achieved by reducing pore size rather than simply improving hydrophilicity [35]. In addition, 1D pores tend to maximize capacity for a given pore size [56]. Among the 20 selected MOFs, there are 11 Al-MOFs and 5 Zr-MOFs. Al-MOFs are ideal for AAWH application because of their stability, non-toxicity, light specific weight, and low cost [53,57]. Also, in terms of scalable synthesis, Al-MOFs have shown a yield that exceeds other MOFs [9]. MOFs not only exhibit reversible adsorption–desorption in the range of 10%–30% RH, but also feature excellent cycle stability. Some Al-MOFs exhibit no performance degradation over thousands of adsorption–desorption cycles, which is a very important property, as the cyclic stability of a material cannot be accurately determined from structural information.

2.3. COFs

COFs, as crystalline porous materials assembled through covalent bonds, have shown extensive application value. COFs feature unique properties, including high porosity, regular structures, and tunable pores [58], and exhibit desirable properties for AAWH: metal-free, avoiding the release of toxic metal ions; moderate affinity for water molecules, facilitating the capture and easy release of water; and regular channels, facilitating the diffusion of water molecules. Although COFs are in the early research stage for water harvesting, the diversity of structures, enabled by the development of structural units and connection chemistry, allows for the fine-tuning of COFs' chemical and geometric structures to achieve water adsorption properties suitable for water harvesting applications.

A COF used for atmospheric water harvesting must first ensure its water stability. Since Lewis acidic sites are easily attacked by water molecules, COFs with B–O bonds are not water stable [59]. As the C=N bond is a stable 8-electron structure, C=N-linked COFs generally exhibit good water stability and can be more resistant to hydrolysis. Among them, the imine-based COFs demonstrate enhanced water stability through their pH-induced reversible formation mechanism, and their stability under acidic conditions can be achieved by enhancing interlayer stacking [60]. COF-432, composed of an extended imine-linked network, features a 1D pore structure with a diameter of 0.75 nm and S-shaped isotherms (Fig. 2(c)), and remains stable over 300 adsorption–desorption cycles [61]. The C–N bond is a saturated bond with excellent stability, where the β-ketoenamine bond, with an irreversible reaction path, exhibits significant water stability [60]. A series of β-ketoenamine-linked COFs were prepared by condensing functionalized aromatic amines with aldehydes, and their isotherms were tested, in which TpPa-1, TpPa-2, and Tp-azo remain stable during five adsorption–desorption cycles [62]. DHTA-Pa containing β-ketoenamine bonds showed no significant attenuation in the adsorption capacity and kinetics of water for up to 80 adsorption–desorption cycles [18]. Other bonded COFs, such as azoles, squaraines, phenazines, and pyrazines, also exhibit significant chemical stability toward water and are promising absorbents for AAWH [8]. With different chemical bonds, COFs can be built with stable performance by adjusting their chemical structure and polarity.

COFs have a variety of topological structures and can be divided into two dimensional (2D) COFs with 1D pore structure and 3D COFs with 3D pore structure according to their spatial extension [63]. As for 2D COFs, symmetric organic building blocks polymerize and expand via covalent bonds into monolayers that overlap through non-covalent interactions, such as Van der Waals forces, π–π stacking, and hydrogen bonding. 2D COFs usually have 1D vertical channels that accelerating the diffusion of water molecules [8]. Their pore shapes can be polygons, and the pore diameter is generally in the range of 0.6–10 nm [64]. Due to the ease of forming interpenetrating networks, pore sizes of 3D COFs are usually in the micropore range [8]. Although the interpenetrating cavities of the 3D COFs' network promote the complete exposure of polar sites to attract water, it would be accompanied by an increase in transport resistance, causing slow water diffusion [8,18]. Currently, only Zhu et al. [65] have reported a 3D COF, 3D-CageCOF-1, in which the –OH groups point into the pores, creating a polar pore environment that enables steep water uptake at p/p_0 = 0.30 (Fig. 2(c)).

Like MOFs, COFs with effective pore sizes larger than the critical diameter of water usually exhibit capillary condensation (20.76 Å at 25 °C) [8], which are characterized by hysteresis loops between the branches of adsorption and desorption isotherms [9], and are not conducive to achieving efficient water harvesting circulation. The water adsorption behavior of hydrophilic COFs with micropores (diameter < 20 Å) generally obeys the following mechanism similar to MOFs: ① nucleation around polar hydrophilic sites [66], ② physical adsorption as clusters or layers, and ③ pore filling. Nucleation on hydrophilic sites is not necessary for some hydrophobic COFs, such as COF-432 [9,61], as they initially form isolated water clusters and then fill the pores immediately after the inflection point ($p/p_0 \geq 0.4$). Obviously, the hydrophilic and hydrophobic properties of COF have a significant impact on its water adsorption properties.

Adjusting the hydrophilicity and hydrophobicity of 2D microporous COFs is vital for the rational design of highly performing AAWH adsorbents. Functionalization of the COF framework can directly adjust its hydrophilicity and hydrophobicity. Twelve stable functionalized Schiff base COFs were prepared by Biswal et al. [62] through functional modification, and the impact of their functionalization on water adsorption behavior was studied: TpPa-1 displays relatively high water uptake and S-shaped isotherms with an inflection point at p/p_0 = 0.24 (Fig. 2(c)), while the hydrophobicity of $-CH_3$, –F, and $-NO_2$ result in the higher inflection point. Stegbauer et al. [67] prepared two azine-linked COFs, azine-benzene-COF (AB-COF) and azine-triformylphloroglucinol-COF (ATFG-COF), which feature isostructural topologies but different skeleton polarities by precisely tuning the chemical properties of the pores. AB-COF exhibits S-shaped isotherms with an inflection point at p/p_0 = 0.24 (Fig. 2(c)). ATFG-COF has more polar oxygen and nitrogen sites, and its isotherm is not steep but features a gradual uptake. In addition to directly synthesizing COFs with various functional groups, post-synthesis transformation is an effective method for adjusting the water adsorption properties of COFs without compromising the microporous structure [68]. Nguyen et al. [69] prepared three hydrazide-linked COFs via post-oxidation of the hydrazine bond and demonstrated that even a slight structural change caused by a small amount of oxidation would lead to a significant shift in the inflection point of the water adsorption isotherm, while attenuating the steepness of the isotherm. The introduction of appropriate heteroatoms or polar functional groups into COF can promote the nucleation around polar

hydrophilic sites, thereby improving its water adsorption capacity at lower relative pressures. Excessive polarity would lead to uniform adsorption of water, thereby losing the steep isotherm. In addition, the increase in the hydrophilicity of COFs could lead to an increase in the isosteric heat, resulting in difficulty in regeneration [70]. The balance of hydrophilic and hydrophobic entities in COFs helps build mild water interactions. Due to the diversity of organic monomers, designing COFs with a hydrophilic and hydrophobic framework containing a variety of functional groups and pore sizes is not difficult [71]. Deliberately designed *ortho*-ketoenamine linked COF (COF-ok), in which dione and naphthalene functionalities act as hydrophilic and hydrophobic entities, respectively, exhibits S-shaped isotherms, an inflection point at p/p_0 = 0.32 (Fig. 2(c)), and a low regeneration temperature of about 45 °C [72]. DHTA-Pa, in which hydrophilic ketone groups and hydrophobic benzene rings are alternatively arranged, features S-shaped isotherms, an inflection point at p/p_0 = 0.26 (Fig. 2(c)), and a lower regeneration temperature at 40 °C [18].

Despite advances in the design and functionalization of COF structures, significant challenges remain to be overcome. From the perspective of COF synthesis, it is required to rationally arrange hydrophilic sites and control the pore size within 2 nm. Furthermore, 1D pore channels with well-aligned hydrophobic and hydrophilic functionalities and appropriate strengths between adsorbents and water molecules are crucial for improving water transport kinetics [18]. There is an urgent need to improve the water uptake of COFs under low relative humidity (< 10% RH), which is essential for employing them in arid regions, such as deserts. Without sacrificing adsorption capacity and kinetics, increasing the proportion of hydrophilic sites or forming a strong interaction between functional groups and water molecules is a potential approach. Finally, it is necessary to expand the scale of COF preparation and conduct in-depth research on COF adsorbent modules used for devices to achieve practical application of COF-based atmospheric water harvesting.

2.4. HOFs

HOFs, which are entirely constructed through multiple hydrogen bonding interactions and other non-covalent interactions such as π–π stacking [73,74], represent a novel category of porous crystalline materials. Owing to the reversibility and flexibility of hydrogen bonds (H-bonds), HOFs can be synthesized under mild conditions and are readily regenerated. Compared with zeolites, MOFs, and COFs, the bonding mode within HOFs is more flexible and relatively weak, and it is understandable for the HOFs' relatively low stability. Good hydrothermal stability is the first requirement for applying HOFs in AAWH. In this context, the synergistic effect of multiple hydrogen bonding and π–π stacking between organic monomers in the HOF's building unit makes it stable in the aqueous environment [74]. In addition, increasing the geometric rigidity as well as coplanarity of H-bonded units helps form stable HOFs with permanent porosity [73], which is favorable for water adsorption. However, studies on water vapor adsorption in HOFs are currently limited, and only a few HOFs exhibit S-shaped isotherms.

Although some HOFs, such as UPC-H1–H3 [75], SPA-1 [76], TCPP-1,3-DPP [77], and γ-$1^{C/C}$ [78], have the ability to absorb water, these HOFs do not have the potential to harvest water due to their limited adsorption capacity caused by small pore volume and natural hydrophobicity. By systematic elongation of π-conjugated molecular arms, mesoporous HOF-102 [79] with large 1.3 $cm^3 \cdot g^{-1}$ pore volume exhibits a high capacity of 0.75 $g \cdot g^{-1}$ but with a large hysteresis and a high inflection point at p/p_0 = 0.71.

H-bonds are weaker than coordination and covalent bonds, for which extra supramolecular interactions, such as halogen bonds and π–π interactions, are needed for highly stable HOFs, resulting in difficulties in designing and controlling the framework of HOFs. Hydrogen-bonded porous materials reported by Roques et al. [80] can tune the porosity and precisely control the size and chemical modification of pores within a specific hydrogen bonding framework to control water adsorption properties without altering the reference structural topology. SPA-1(R), in which R=H, CH_3, OH, OH:CH_3, exhibits a tunable inflection point, but the introduction of functional groups would reduce the pore volume and greatly shrink the water adsorption capacity. This indicates that HOFs are less tunable than MOFs, COFs, and zeolites. HOF-BTB [74] features an S-shaped isotherm, an inflection point at p/p_0 = 0.48, and small hysteresis (Fig. 2(a)). Although HOF-BTB has good water stability, its 0.32 $g \cdot g^{-1}$ water capacity decreased by 19.1% after five adsorption–desorption cycles. HOFs currently have low water capacity and poor cycling durability, so there remains a distance before they can be applied to atmospheric water harvesting. Maintaining pore volume and porosity as much as possible while improving the stability of HOF is the key to developing water-harvesting HOF in the future.

2.5. Summary

The structural characteristics and water adsorption properties of selected zeolites, MOFs, COFs, and HOFs adsorbents based on six criteria are summarized. There are significantly more MOFs suitable for atmospheric water harvesting applications than the other three adsorbents, highlighting the advantages of isoreticular chemistry, which enables the desired isotherms to be obtained through the fine-tuning of metal clusters or linkers (Figs. 3(a)–(c)). By comparing Figs. 2(a)–(c), it can be observed that MOFs exhibit typical step-like S-shaped isotherms without hysteresis, and the water uptake basically reaches saturation near the inflection point. As shown in Fig. 2(d), the inflection points of MOFs are located in the arid range of p/p_0 = 0.1–0.3, which are lower than those of most COFs and HOFs, and the water capacities of MOFs are larger than those of zeolites. Furthermore, most MOFs have no performance degradation over dozens to thousands of adsorption–desorption cycles. MOFs have achieved a good balance between high water capacity and low inflection point (Figs. 2(d) and 3(d)), so it is understandable that a variety of MOF-based water harvesting devices have emerged.

As for most zeolites, MOFs, COFs, and HOFs with steep S-shaped isotherms without hysteresis, their water adsorption follows three stages: initial adsorption at specific sites, formation of water clusters, and pore filling. These four types of materials have significantly different initial adsorption sites, resulting in their different adsorption behaviors (Figs. 2(a)–(c) and (e)). The strong hydrophilic sites of zeolite materials promote initial adsorption at low relative pressures, accompanied by a high adsorption heat, which requires more energy-intensive regeneration. Open metal sites and the polar (hydrophilic) groups of organic linkers are regarded as initial nucleation sites for MOFs. The rich variety of initial sites endows MOFs with highly adjustable water adsorption behavior, especially allowing for the tuning of the inflection point. COFs and HOFs have relatively high initial adsorption pressures and inflection points due to the natural hydrophobicity of pure organic frameworks. Although HOFs display reversible pore filling, they are less durable than the other three materials due to the flexibility of the framework.

By summarizing in Table 1 [4,11,16–18,29,31,38–42,46–55,61,62,65,67,72,74,81–84], Fig. 2, and the adsorption mechanism, some design criteria of structural characteristics can be derived. The pore size is directly related to the pore volume and the position of the inflection point, and a pore size of about 1 nm appears to be a suitable choice. In addition to the pore size, the regular structure of the

Table 1
Structural characteristics and water adsorption properties of selected adsorbents.

Type	Material	Linker or monomer	α [-][a]	q_{max} [g·g^{-1}][b]	d_{pore} [Å][c]	Pore space	ρ_c [g·mL^{-1}][d]	$-\Delta_{ads}H$ [kJ·mol^{-1}][e]	V_p [cm^3·g^{-1}][f]	Stability	Refs.
Zeolites	AlPO-42	—	0.13	0.42 (303 K)	2.5, 4.2, 6.3, 11.0	3D	1.412	69–46	—	Less than 2% loss in q_{max} after 40 ads.[g] cycles	[31]
	EMM-8	—	0.15	0.39 (303 K)	7	1D	1.5	46.76	0.59	3.3% loss in Δq over 30 ads. cycles	[81]
	DNL-11	—	0.05	0.37 (303 K)	6.5	1D	—	—	—	Constant Δq over 13 ads. cycles	[29]
	AQSOA-Z01	—	0.19	0.20 (308 K)	7.4, 8.3	1D	1.75	56.1	—	—	[11,82]
	AQSOA-Z05	—	0.30	0.21 (308 K)	7.4, 8.3	1D	1.75	52.6	—	—	[11]
Metal–organic framework (MOF)	Ni_2Cl_2(BTDD)	BTDD	0.29	1.14	22	1D	0.852	—	—	—	[47]
	Co_2Cl_2(BTDD)	BTDD	0.29	0.97	22	1D	0.69	55–41	—	6.3% loss in Δq after 30 ads. cycles	[46]
	MOF-LA2-1 (Al) (pyrazole)	PZVDC	0.26	0.64	11	1D	0.847	65.8–47.3	0.67	Constant Δq over 150 ads. cycles	[17]
	MIP-211(Al)	*t,t*-muconate	0.29	0.61	8.5	1D	0.807	48.6–45.5	0.60	Constant Δq over 40 ads. cycles	[53]
	MOF-LA2-2 (Al) (furan)	FDP	0.31	0.57	11.1	1D	1.148	50	0.597	Constant Δq over 165 ads. cycles	[51]
	MOF-841(Zr)	MTB	0.22	0.51	13.3	3D	1.05	58–42	0.53	7% loss in q_{max} after 5 ads. cycles	[40]
	Zr-adip	ADIP	0.11	0.48	6.6, 12.8	1D	1.17	51–46	0.47	Constant Δq over 300 ads. cycles	[49]
	MOF-LA2-1 (Al) (furan)	FVDC	0.14	0.47	9.2	1D	—	53	0.433	Constant Δq over 165 ads. cycles	[51]
	MOF-303(Al)	PZDC	0.13	0.45	6	1D	1.159	50–40	0.54	Constant Δq over 150 ads. cycles	[4]
	MIL-125(Ti)-NH_2	NH_2-BDC	0.2	0.45	6, 12	3D	0.81	—	0.51	—	[50]
	Al-fumarate	FA	0.27	0.45	5.7 × 6.0	1D	1.24	50–42	0.48	Constant Δq over 4500 ads. cycles	[38]
	MIP-200(Zr)	MDIP	0.18	0.45 (303 K)	13, 6.8	1D	1.16	70–45	0.40	6% loss in Δq over 1–10 ads. cycles and constant Δq over 10–40 ads. cycles	[48]
	MOF-333(Al)	FDC	0.22	0.45	9.4	1D	1.122	52.7–46.8	0.523	-	[16]
	KMF-1(Al)	PyDC	0.16	0.43 (313 K)	5.7	1D	1.08	57–52	0.473	Constant Δq over 50 ads. cycles	[55]
	CAU-23(Al)	TDC	0.27	0.42	7.6	1D	1.07	48.2	0.48	Constant Δq over 5000 ads. cycles	[39]
	Zr-Fum HT	FA	0.10	0.41 (313 K)	5.8, 11.2	3D	1.59	52–45	0.553	Constant Δq over 50 ads. cycles	[41]
	MIL-160(Al)	FDC	0.09	0.38 (303 K)	5	1D	1.068	64–43	0.40	Constant Δq over 10 ads. cycles	[54]
	CAU-10(Al)-H	1,3-BDC	0.16	0.37	7	1D	1.15	53.5	—	Constant Δq over 9 ads. cycles	[83]
	MOF-801(Zr)	FA	0.09	0.36	4.8, 5.6, 7.4	3D	1.68	62–47	0.45	Stable over 5 ads. cycles	[40]
	Co-CUK-1	PDC	0.12	0.30 (303 K)	13.4 × 13.0	1D	1.46	60–45	0.26	Constant Δq over 50 ads. cycles	[42]
Covalent organic framework (COF)	DHTA-Pa	Pa	0.26	0.71	14	1D	—	51–44	—	Constant Δq over 80 ads. cycles	[18]
	COF-ok	2,3-DHNA	0.32	0.62	13	1D	—	49.8	—	Constant Δq over 20 ads. cycles	[72]
	TpPa-1	Pa	0.24	0.44	18	1D	—	—	—	Constant Δq over 5 ads. cycles	[62]
	AB-COF	TFB	0.24	0.41 (288 K)	13	1D	—	49.4	0.50	—	[67]
	3D-CageCOF-1	DHTPA	0.30	0.32	5.6, 8.8	3D	—	49.6	0.50	8% loss in q_{max} after 3 ads. cycles	[65]
	COF-432	TFB	0.35	0.30	7.5	1D	0.875	48	0.43	Constant Δq over 300 ads. cycles	[61]
Hydrogen-bonded organic framework (HOF)	HOF-BTB	BTB	0.48	0.32	16.6[h]	1D	—	—	0.40	19.1% loss in q_{max} after 5 ads. cycles	[74,84]

[a] α represents the inflection point of the water uptake step, the relative pressure for which the capacity is 50% of q_{max}.
[b] q_{max} represents the maximum water uptake capacity (under 298 K unless otherwise stated), Δq represents water uptake capacity.
[c] d_{pore} represents size of aperture or cage window.
[d] ρ_c represents crystal density.
[e] $-\Delta_{ads}H$ represents heat of adsorption (isosteric heat or average of isosteric heat).
[f] V_p represents pore volume, derived from 77 K N_2 adsorption.
[g] ads. represents adsorption.
[h] Mean pore diameter.

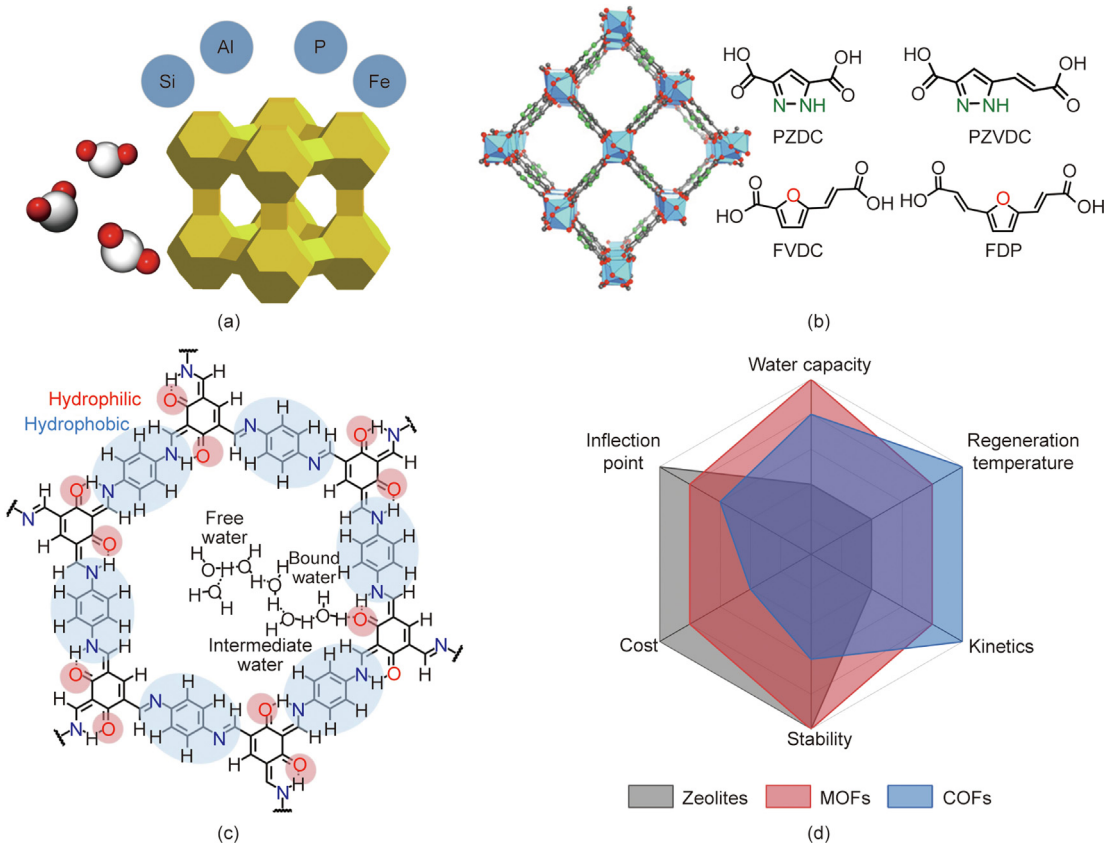

Fig. 3. (a) Developing analogous materials with different chemical compositions for a certain zeolite framework could exhibit better water adsorption properties. (b) Isoreticular expansion strategy for MOFs: By synthesizing MOFs with specific SBUs using linkers varying in sizes, lengths, or side chains, one can obtain frameworks with similar networks but diverse pore sizes and environments [4,17,51]. PZDC represents 1*H*-pyrazole-3,5-dicarboxylic acid. PZVDC represents (*E*)-5-(2-carboxyvinyl)-1*H*-pyrazole-3-carboxylic acid. FVDC represents (*E*)-5-(2-carboxyvinyl)-2-furancarboxylic acid. FDP represents (*E*,*E*)-3,3′-(2,5-furandiyl)*bis*-2-propenoic acid. Reproduced from Ref. [4] with permission. (c) Taking DHTA-Pa as an example, the pore environments can be adjusted through alternatively arranged hydrophilic sites and hydrophobic segments. Reproduced from Ref. [18] with permission. (d) Evaluate zeolites, MOFs, and COFs from six major evaluation dimensions of inflection point, water capacity, regeneration temperature, kinetics, stability, and cost. Variables further from the center represent low inflection point, high water capacity, low regeneration temperature, fast kinetics, high stability, and low cost.

pores also creates favorable conditions for the formation of highly organized water clusters under low relative pressure [9,11]. The rational design of the pore structure and its surface chemistry helps to achieve a balance between adsorption capacity and energy consumption required for desorption. Appropriately decorated with the right number of strongly hydrophilic sites in relatively hydrophobic pores to avoid the formation of a uniform, strongly hydrophilic pore surface seems to be a feasible strategy. Considering the structural similarity of straight and regular pore channels within 1D porous organic frameworks, the regular distribution of hydrophilic and hydrophobic sites within the channel facilitates the formation of regular water clusters, which is beneficial for the formation of steep isotherms (Fig. 3(c)). For organic frameworks with a 3D pore structure, their internal shapes are often irregular, such as 3D interconnected pocket-like cavities in MOF-801(Zr) [40]. The interpenetrating cavities of the 3D network promote complete exposure of polar sites, resulting in higher energy barriers for water diffusion and thereby increasing the diffusion resistance of water [8,18]. In addition, some MOFs with 2D pore structures feature S-shape isotherms, such as MWH-1(Zn) (MWH represents MOF for water harvesting) [85] and Cr-mos-MOF-1 [86], but their application in AAWH is limited by a low water capacity and by a large hysteresis loop, respectively. Although materials with 1D regular channels currently exhibit good water adsorption properties, ideal straight-through and regular 2D and 3D channels with high connectivity are still worth further exploration. Besides, different adsorbents perform optimally at varying humidity levels. Therefore, designing mixed or composite materials in various forms (such as physical mixing, layered structures, and core–shell structures) is expected to maximize water adsorption under a wider range of environmental conditions.

As a bridge connecting materials and engineering, obtaining sufficient adsorbent materials at an affordable price is the key to promoting AWH technology. Directly synthesizing adsorbents with desired water sorption properties without post-modification can simplify the synthesis process and reduce cost. In addition to conventional commercial zeolites, Al-MOFs with exceptional water adsorption characteristics have demonstrated the potential for industrial-scale batch production owing to their cost-effective aluminum feedstock and environmentally friendly production processes, which substitute organic solvents with water-based protocols [87–89]. The diversified linker modification strategies also give Al-MOFs a wider expansion. The scale-up production of Al-MOFs, such as MOF-303, Al-fumarate, CAU-23, MIL-160, and CAU-10, is no longer a challenge [85]. However, it is necessary to take into account the large-scale and affordable production of ligands required for MOF-333 and some linker-extended Al-MOFs. While novel adsorbents demonstrate exceptional water capacity and a low inflection point under controlled laboratory conditions, a comprehensive assessment of their scalability, long-term stability in practical operating environments (e.g., exposure to airborne particulates and environmental temperature

fluctuations), and economic viability is imperative to determine their feasibility for real-world applications.

3. Engineering device aspects

3.1. Adsorbent component design

Optimizing the performance of an AAWH device involves focusing on two key areas: adsorbents and engineering component-level properties [32]. Although the water adsorption isotherm defines equilibrium capacity, the actual performance of AAWH systems cannot be solely reflected by such equilibrium characteristics, as the resistance related to heat and mass transfer in bulk materials can limit system performance. The heat (energy) and mass transport characteristics are essential for determining system productivity and effectiveness. Water adsorption–desorption kinetics of bulk adsorbents depend on intra-crystalline and inter-crystalline vapor diffusion, making it crucial to optimize crystal size, shape, porosity, and packing density.

For zeolites, MOFs, and COFs discussed above, which are the state-of-the-art adsorbents with affinity for water molecules, their apparent water vapor adsorption rates do not differ by more than one order of magnitude [5,18]. In terms of desorption kinetics, MOFs, such as MOF-303(Al) and Al-fumarate [5], and COFs, such as DHTA-Pa and COF-ok [18,72], have obvious advantages. Unfortunately, there are currently no kinetic studies on HOFs. Hot surface heating with solar and/or electricity is currently the common method employed to drive adsorbents to release adsorbed water [9]. Increasing the heat transfer rate can directly enhance water yield, but improving the heat transfer often has a direct trade-off with mass transfer. For example, increasing packing density boosts heat transfer but restricts vapor movement. Constructing composite adsorbents by purposefully embedding functional components, such as carbon or metal foams [14,90,91], magnetic nano-particles [92], carbon paper or fibers [91,93], and MXene nanosheets [94], or incorporating small amounts of highly thermally conductive materials, can promote heat transfer with minimal effects on the mass transfer. When embedded functional components are exposed to external stimuli like magnetic fields, electrical currents, light, or combinations thereof, rapid and uniform heating can be generated within the adsorbent. This strategy is widely employed in devices that utilize MOFs and zeolites as adsorbents [9,32].

3.2. AAWH device design

Optimal AAWH system design on energy and productivity demands multi-scale integration of adsorption thermodynamics (scale-independent) and heat and mass transport (scale-dependent), both at the bulk adsorbent level and the device level. Therefore, in terms of engineering device aspects, it is necessary to design the loading method of adsorbents and the operation mode of the device reasonably based on the adsorption–desorption cycle capacity and adsorption and desorption kinetics of each adsorbent. AAWH devices are categorized by passive monocyclic devices and active multicyclic devices based on their operational frequency and water release and condensation methods [36]. Passive monocyclic devices exploit relative humidity fluctuations caused by daily temperature changes. At night, the device adsorbs water vapor. During the day, the saturated adsorbent is heated by direct solar radiation, thereby releasing the adsorbed water, which is then condensed and collected. For adsorbents with slow kinetics but good water capacity, passive monocyclic devices can maximize their adsorption capacities and theoretically do not require external energy input. On the contrary, adsorbents with faster kinetics and the ability to reach saturation in a few hours or less are suitable for multi-cycle operations within a day. Active multicyclic AAWH devices enhance water collection by performing multiple adsorption–desorption cycles throughout the day, surpassing the limitations of passive monocyclic devices, but require the introduction of additional energy to allow the adsorbents to release water.

3.3. Progress in AAWH devices

Various MOFs exhibit superior water adsorption/desorption properties and stability, making them ideal for AAWH from arid air [5,36]. MOF-based passive monocyclic AAWH device can already produce drinking water without the need for external energy sources aside from ambient sunlight [91]. As shown in Fig. 4, a MOF-801(Zr) based device with the condenser positioned on the sidewalls and a reflector added to the casing to reduce condensation, exhibited a daily productivity of 0.1 liter per kilogram of MOF material ($L{\cdot}kg_{MOF}^{-1}$) in the Arizona Desert (Fig. 4(a)) [4]. Condensing and collecting as much of the water vapor released by the adsorbents as possible by incorporating some clever design of heat and mass transfer, such as increasing airflow circulation and lowering the condensation temperature [95], is critical to maximizing the water productivity. The innovative coupling of a passive monocyclic AAWH device with thermoelectric power generation (TEPG) and nighttime radiative cooling significantly boosted both power density (~346%) and water production (up to 0.93 $L{\cdot}kg_{MOF}^{-1}{\cdot}day^{-1}$) [90]. A novel cylindrical device (Fig. 4(b)) equipped with a MOF-303(Al) cartridge, which utilized thin disc-shaped pellets made from MOF powders stacked with porous nickel foam discs to efficiently distribute heat during desorption, could produce 0.285 and 0.210 $L{\cdot}kg_{MOF}^{-1}$ of water a day in Berkeley and Death Valley National Park, respectively [91]. Enhancing water production requires MOFs with high uptake at low relative humidity, which often demand higher regeneration temperatures. Cooling-assisted sorption-enhanced atmospheric water harvesting (CSAWH) can improve performance by increasing effective RH near the adsorbent [96], despite additional cooling and a low solar energy conversion rate.

Solar-driven water release passive monocyclic AAWH devices exhibit low daily productivity per solar absorber area, and their heat and mass transfer need to be enhanced. LaPotin et al. [14] proposed a dual-stage atmospheric water harvesting device (Fig. 4(e)) employing commercial zeolite AQSOA-Z01. The two stages increased the daily productivity per solar absorber area of ~0.77 $L{\cdot}m^{-2}$ by recycling the latent heat of condensation from the top stage to facilitate desorption in the bottom stage. The dual-stage approach can be used with other high-performance adsorbents and extended to various AAWH systems for enhanced thermal efficiency. Although using a two-stage approach can increase thermal efficiency to a certain extent to make up for the low thermal conductivity of the air between stages, the daily productivity per unit mass of adsorbent (0.115 liter per kilogram of zeolite material ($L{\cdot}kg_{zeolite}^{-1}$)) is lower than that of a single-stage device (0.167 $L{\cdot}kg_{zeolite}^{-1}$) [14]. Therefore, improving thermal conductivity without compromising system kinetics remains a challenging task.

As for active multicyclic AAWH devices, an active device employed MOF-303(Al), as shown in Fig. 4(c), achieved a daily productivity of ~1.3 $L{\cdot}kg_{MOF}^{-1}$ [5], significantly higher than the ~0.1 $L{\cdot}kg_{MOF}^{-1}$ reported by the same team for the passive device [4]. These active devices use electric and/or solar heating for mild heating to facilitate water release. Compared with passive devices, this method boosts productivity by an order of magnitude while also placing higher requirements on the cycle stability of the adsorbents. Rapid cycling that utilizes the partial working capacity of MOFs will help increase the overall water productivity by

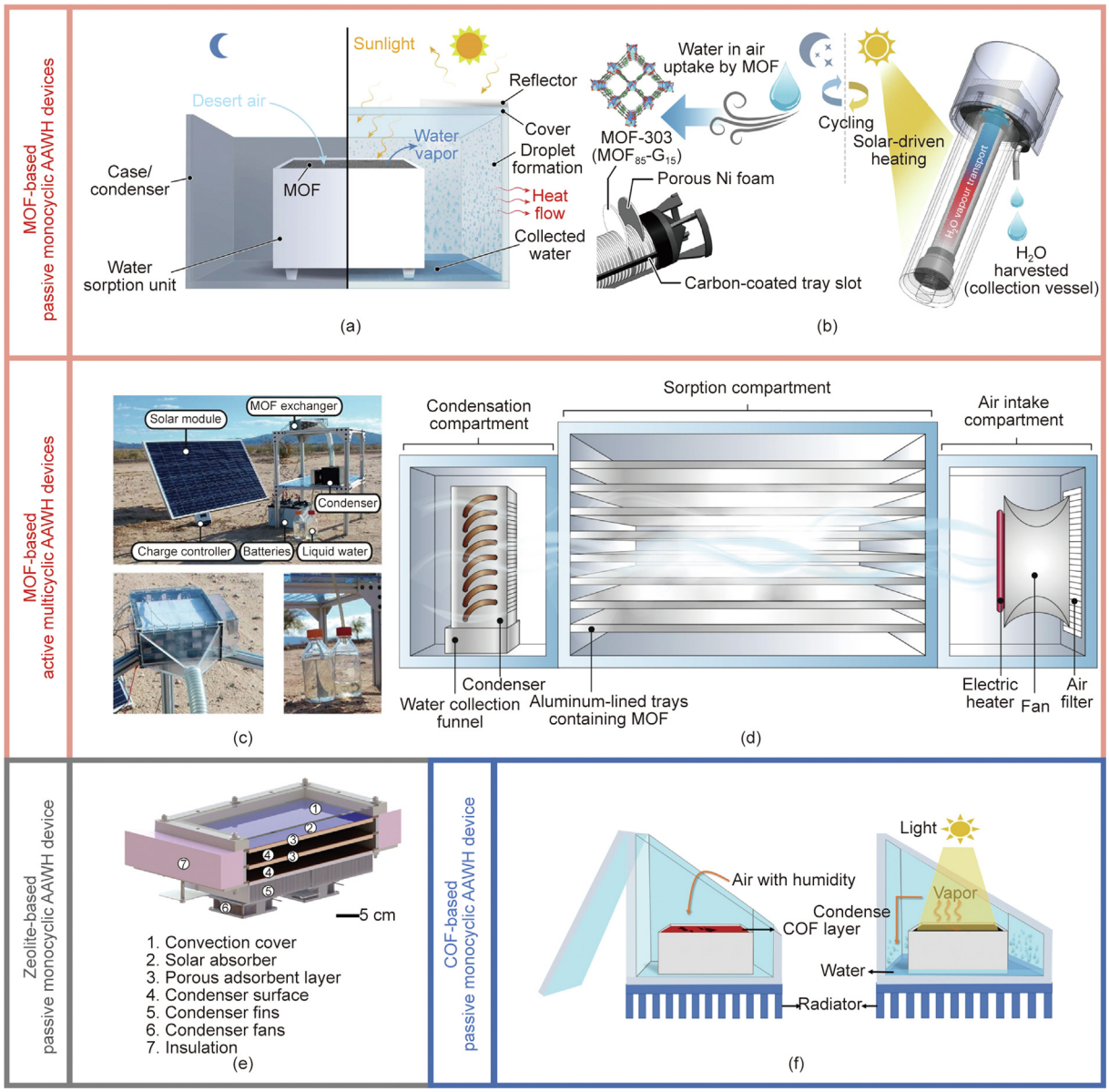

Fig. 4. MOF-based passive monocyclic AAWH devices: (a) Scheme of a device comprising a water adsorption unit and a condenser case [4] and (b) scheme of a cylindrical device designed to optimize solar energy utilization from sunrise to sunset [91]. MOF-based active multicyclic AAWH devices: (c) scheme of a device in the Mojave Desert [5] and (d) scheme of an adaptive device to improve its daily productivity with controllable time consumed per cycle [98]. (e) Zeolite-based passive monocyclic AAWH device with dual-stage design [14]. (f) COF-based passive monocyclic AAWH device [72]. Reproduced from Refs. [4,5,14,72,91,98] with permission.

optimizing the uptake-release cycle time [97]. Adaptive water harvesting devices that using electric heated hot flow to trigger water release (Fig. 4(d)), like the one made by Almassad et al. [98] with MOF-801(Zr), adjust cycles based on real-time weather conditions, improving daily productivity from 1.2 to 2.4 $L{\cdot}kg_{MOF}^{-1}$ at 10%–30% RH, and even further doubled for 30%–60% RH conditions.

Atmospheric water harvesting devices based on COF are still in the laboratory stage, with only a few devices having been reported to date [72]. To verify the water capacity of COF-ok, Chen et al. [72] designed the passive monocyclic AAWH device shown in Fig. 4(f). The device exhibits a daily productivity of 0.161 $L{\cdot}kg_{COF}^{-1}$, and the produced water meets the standards proposed by the World Health Organization, which demonstrates the potential application of COF-based atmospheric water harvesting.

MOF-based AAWH has shown promising daily water production levels, but more competitiveness is needed. Efforts should focus on practical applications, beginning with large-scale MOF production, and sub-tonne level high-performance MOFs are being produced [99]. Fabricating MOF powders into pellets [100] or films [15] through suitable binders requires the preservation of crystallinity and porosity, while the decrease of water loading triggered by the equivalent mass of binder added is inevitable [101]. In addition, water condenses in the interparticle space between bulk MOF crystals, creating extra uptake and hysteresis in isotherms [102]. Considering the ultrafast kinetics of single MOF crystals and the potential desorption hysteresis in the bulk MOF, this effect can be minimized by using MOF particles with crystal sizes of 10–20 μm, in which intra-particle diffusion is negligible [102], or by employing fluidization-based devices where water adsorption happens in isolated particles [103]. In summary, a passive monocyclic AAWH device can already produce water without an additional source except for the sun. However, the complex relationship between energy input and water yield, such as the water–energy nexus, must be

addressed to improve the energy utilization efficiency of active devices. Suggested strategies include using highly thermally conductive composites, radiative cooling, cooling-assisted adsorption, and adapting harvesting cycles based on weather or seasonal changes. At present, the synthesis cost of COFs is still higher than that of MOFs and zeolites [70,86]. Therefore, only by establishing a large-scale and low-cost COF production process can COFs be widely used in actual devices.

3.4. Summary

In terms of device development, the use of MOFs and zeolites to harvest atmospheric water has been demonstrated in medium-sized AAWH devices, which reach the indicative technology readiness level (TRL) [104] of 7–8 [9]. Limited by the yield and cost of COFs, the development of COF-based AAWH devices is still in an early stage. Unlike commercially available "hydropanel" based on unknown adsorbents [105], the currently reported devices based on MOFs and zeolites still exhibit inadequate daily water productivity to meet an adult's daily water requirement of ~4 L [96]. If active devices could double current production, it would gain a lot of attention and accelerate their adoption. For passive devices, it is relatively challenging to increase the water production capacity per unit mass of adsorbent. The integration of adsorbent composite assemblies with high-efficiency photothermal conversion materials is an aspect that warrants attention [106]. In addition, the advanced condensation technology has the potential for system integration in AAWH devices. For example, a well-designed radiative cooling assembly can not only enable passive gravity-driven water collection [107], but also can condense the water vapor released by the adsorbent into liquid water under direct sunlight without energy consumption [108]. The next generation of AAWH devices should be designed to operate large quantities of adsorbents, utilizing rationally shaped materials and structural arrangements to optimize heat removal (adsorption) and supply (desorption), accelerate water vapor transfer, and be able to collect several liters of liquid water per day to meet human needs.

4. Conclusions and perspectives

Advances in water vapor adsorbents have triggered extensive research into atmospheric water harvesting technologies and applications. Although the concept of AAWH has been fully demonstrated, the development of high-performance adsorbents and devices remains a prerequisite for their wide application. Zeolites, MOFs, COFs, and HOFs are ideal adsorbents for AAWH because of their steep S-shaped isotherms. In the summary of this review, we focus on the above four types of materials that possess steep isotherms in the arid range. Regular micropores are conducive to the formation of steep isotherms without hysteresis, and the reasonable arrangement of hydrophilic and hydrophobic sites in the pores is conducive to controlling the timing of pore filling. Overall, MOFs are the most ideal in terms of diversity, isotherm shape, inflection point, and water capacity, and their steep uptake at the inflection point is beneficial for water harvesting applications. Molecular simulation studies can reveal the influence of linker changes [17] and hydrophilic site distribution [109] on water adsorption properties of MOFs. Advanced molecular simulation methods enable high-throughput screening of existing massive MOF datasets [110,111] and further discovery of more candidates with potential in water harvesting [112]. Besides, there is a clear relationship between the structure of MOF and water adsorption performance, especially regarding isotherms as well as water capacity [56], which makes artificial intelligence (AI)-assisted MOF design possible. For a given MOF structure, machine learning methods can be employed to accurately predict its water adsorption isotherm [113,114]. In addition, datasets of MOF linkers have been established, and the GPT model is used to innovate the MOF linker structure designs [115]. By using data-driven algorithms to predict adsorption properties and identify potential candidates, AI is anticipated to accelerate the exploration of adsorbents with various dimensional structures. It is worth noting that hydrolysis can be readily forecasted based on fundamental chemical principles and steric effects. However, accurately predicting structural stability against capillary forces exerted on pore walls during water desorption remains challenging, and experimental determination is needed [36]. For the future development of efficient AAWH adsorbents, water adsorption–desorption cycle experiments are indispensable. Adsorbents that can maintain stability in hundreds or thousands of cycles can greatly reduce the cost of use in practical applications.

The issue of the water–energy nexus is a specific topic for the design and construction of AAWH devices. The reliability and safety of solar energy make it an ideal energy source for AAWH, and water-scarce areas tend to have abundant solar resources. An efficient solar energy capture and conversion system is crucial for the efficient operation of AAWH devices. By compounding MOF with highly thermally conductive materials, a new generation of passive MOF AAWH devices can harvest water under extremely arid desert conditions with only solar energy input [91], which broadens the regions of applicability of AAWH devices, such as developing regions without an electricity grid. In addition, active AAWH devices, which can use electrical heating, external waste heat, or other sustainable heat sources in conjunction with daytime solar energy, possess higher water productivities and the ability of operating in various weather conditions. Therefore, water production and energy efficiency of active devices can be optimized by intelligently adjusting or integrating energy sources according to environmental conditions and operational needs [97,98].

Optimization of the heat and mass transfer characteristics [11] of devices, as well as the integration of components, is of importance to improve their water productivity and efficiency, especially for active devices. Multi-scale engineering of heat and mass transfer is of significance in realizing efficient water production cycles. However, preparing adsorbent assemblies with efficient adsorption–desorption kinetics while ensuring high thermal efficiency has always been a difficult problem. Porous and honeycomb characteristic structures [116], like in catalysis engineering [117–119], are probably the way to go. Determining the adsorption–desorption kinetics of bulk adsorbents or adsorbent assemblies is encouraged, as the heat and mass transfer in bulk samples testing is closer to the actual operating conditions for effective device-level evaluation [120]. Considering it from another perspective, tailoring the operating strategy of active devices to suit the adsorbent's kinetic profile can maximize performance. In terms of system design of AAWH devices, by establishing numerical models of heat and mass transfer for the devices [11,15,91], the moisture migration path can be more reasonably optimized, thereby improving the performance of the device while reducing production costs and design cycles.

Finally, the advancement of AAWH technology is inseparable from the development of high-performance adsorbents and the design and engineering of efficient devices. Currently, among the four types of porous crystal adsorbent materials: zeolites, MOFs, COFs, and HOFs, only devices based on MOF adsorbents are expected to be commercialized. Several key research gaps deserve more exploration: ① Kinetic studies on HOFs to evaluate their potential in rapid-cycling devices. ② Evaluating the construction cost of composite adsorbent assemblies for enhanced heat transfer. ③ Developing methods for maintaining porosity in MOF/COF

pellets or films, such as binder-free formulation. ④ Scientific design of large-scale adsorption components and devices to further increase water yield. ⑤ Energy recovery integration of water harvesting devices on the system level. ⑥ Techno-economic and life cycle assessment analyses for scale-up AAWH application. In addition, the water collected by AAWH is not only limited to drinking, but can also be used for agricultural drip irrigation [121] and clean energy production [122], which expands the scope of AAWH technology. In the future, in addition to providing fresh water, AAWH technology could be integrated into passive cooling, dehumidification, and power generation systems, in line with the wider goals of green and low-carbon.

CRediT authorship contribution statement

Bo Zhang: Writing – original draft, Methodology, Investigation, Data curation, Conceptualization. **Zhi Wang:** Methodology. **Freek Kapteijn:** Writing – review & editing. **Xinlei Liu:** Writing – review & editing, Supervision, Funding acquisition, Conceptualization.

Declaration of competing interest

The authors declare that they have no known competing financial interests or personal relationships that could have appeared to influence the work reported in this paper.

Acknowledgments

This work was supported by the Inner Mongolia Autonomous Region Unveiling Project (2022JBGS0027), the National Key Research and Development Program (2021YFB3801200), and the Seed Foundation of Tianjin University (2024XJD-0058).

References

[1] Meng Y, Dang Y, Suib SL. Materials and devices for atmospheric water harvesting. Cell Rep Phys Sci 2022;3(7):100976.
[2] Tu Y, Wang R, Zhang Y, Wang J. Progress and expectation of atmospheric water harvesting. Joule 2018;2(8):1452–75.
[3] Zhang S, Fu J, Xing G, Zhu W, Ben T. Recent advances in porous adsorbent assisted atmospheric water harvesting: a review of adsorbent materials. Chem Synth 2023;3(2):10.
[4] Fathieh F, Kalmutzki MJ, Kapustin EA, Waller PJ, Yang J, Yaghi OM. Practical water production from desert air. Sci Adv 2018;4(6):eaat3198.
[5] Hanikel N, Prevot MS, Fathieh F, Kapustin EA, Lyu H, Wang H, et al. Rapid cycling and exceptional yield in a metal–organic framework water harvester. ACS Cent Sci 2019;5(10):1699–706.
[6] Kim H, Rao SR, Kapustin EA, Zhao L, Yang S, Yaghi OM, et al. Adsorption-based atmospheric water harvesting device for arid climates. Nat Commun 2018;9(1):1191.
[7] Kim H, Yang S, Rao SR, Narayanan S, Kapustin EA, Furukawa H, et al. Water harvesting from air with metal–organic frameworks powered by natural sunlight. Science 2017;356(6336):430–4.
[8] Sun C, Sheng D, Wang B, Feng X. Covalent organic frameworks for extracting water from air. Angew Chem Int Ed 2023;62(25):e202303378.
[9] Zhang B, Zhu Z, Wang X, Liu X, Kapteijn F. Water adsorption in MOFs: structures and applications. Adv Funct Mater 2024;34(43):2304788.
[10] Han B, Ng MS, Chakraborty A. Optimizing metal–organic frameworks for adsorption-based atmospheric water harvesting: a systematic evaluation of pristine and modified MOFs for enhanced performance in diverse climates. Chem Eng J 2025;521:166607.
[11] Liu X, Wang X, Kapteijn F. Water and metal–organic frameworks: from interaction toward utilization. Chem Rev 2020;120(16):8303–77.
[12] Kalmutzki MJ, Diercks CS, Yaghi OM. Metal–organic frameworks for water harvesting from air. Adv Mater 2018;30(37):1704304.
[13] Zhou XY, Lu HY, Zhao F, Yu GH. Atmospheric water harvesting: a review of material and structural designs. ACS Mater Lett 2020;2(7):671–84.
[14] LaPotin A, Zhong Y, Zhang LA, Zhao L, Leroy A, Kim H, et al. Dual-stage atmospheric water harvesting device for scalable solar-driven water production. Joule 2021;5(1):166–82.
[15] Lassitter T, Hanikel N, Coyle DJ, Hossain MI, Lipinski B, O'Brien M, et al. Mass transfer in atmospheric water harvesting systems. Chem Eng Sci 2024;285:119430.
[16] Hanikel N, Pei XK, Chheda S, Lyu H, Jeong W, Sauer J, et al. Evolution of water structures in metal–organic frameworks for improved atmospheric water harvesting. Science 2021;374(6566):454–9.
[17] Hanikel N, Kurandina D, Chheda S, Zheng Z, Rong Z, Neumann SE, et al. MOF linker extension strategy for enhanced atmospheric water harvesting. ACS Cent Sci 2023;9(3):551–7.
[18] Sun C, Zhu Y, Shao P, Chen L, Huang X, Zhao S, et al. 2D covalent organic framework for water harvesting with fast kinetics and low regeneration temperature. Angew Chem Int Ed 2023;62(11):e202217103.
[19] Thommes M, Kaneko K, Neimark AV, Olivier JP, Rodriguez-Reinoso F, Rouquerol J, et al. Physisorption of gases, with special reference to the evaluation of surface area and pore size distribution (IUPAC technical report). Pure Appl Chem 2015;87(9–10):1051–69.
[20] van der Veen MA, Canossa S, Wahiduzzaman M, Nenert G, Frohlich D, Rega D, et al. Confined water cluster formation in water harvesting by metal–organic frameworks: CAU-10-H versus CAU-10–CH3. Adv Mater 2024;36(12):2210050.
[21] Zhang S, Fu JR, Xing GL, Zhu WD, Ben T. Porous materials for atmospheric water harvesting. ChemistryOpen 2023;12(5):e202300046.
[22] Ejeian M, Wang RZ. Adsorption-based atmospheric water harvesting. Joule 2021;5(7):1678–703.
[23] Herzog TH, Jaenchen J, Kontogeorgopoulos EM, Lutz W. Steamed zeolites for heat pump applications and solar driven thermal adsorption storage. In: Häberle A, editor. Proceedings of the 2nd International Conference on Solar Heating and Cooling for Buildings and Industry (SHC); 2013 Sep 23–25; Freiburg, Germany. Red Hook: Curran Associates, Inc.; 2013. p. 380–3.
[24] Tashiro Y, Kubo M, Katsumi Y, Meguro T, Komeya K. Assessment of adsorption–desorption characteristics of adsorbents for adsorptive desiccant cooling system. J Mater Sci 2004;39(4):1315–9.
[25] Tatlier M, Munz G, Henninger SK. Relation of water adsorption capacities of zeolites with their structural properties. Microporous Mesoporous Mater 2018;264:70–5.
[26] Abd Elwadood SN, Dumée LF, Al Wahedi Y, Al Alili A, Karanikolos GN. Aluminophosphate-based adsorbents for atmospheric water generation. J Water Process Eng 2022;49:103099.
[27] Russina M, Günther G, Grzimek V, Schlegel MC, Veziri CM, Karanikolos GN, et al. Nanoscale dynamics and transport in highly ordered low-dimensional water. J Phys Chem Lett 2019;10(20):6339–44.
[28] Schlegel MC, Grzimek V, Guenther G, Svetogorov R, Veziri CM, Kapsi M, et al. Explaining water adsorption in one-dimensional channels in $AlPO_4$–5 on molecular scale. Microporous Mesoporous Mater 2020;304:109201.
[29] Nie C, Yan N, Liao C, Ma C, Liu X, Wang J, et al. Unraveling a stable 16-ring aluminophosphate DNL-11 through three-dimensional electron diffraction for atmospheric water harvesting. J Am Chem Soc 2024;146(15):10257–62.
[30] Ristić A, Logar NZ, Henninger SK, Kaucic V. The performance of small-pore microporous aluminophosphates in low-temperature solar energy storage: the structure-property relationship. Adv Funct Mater 2012;22(9):1952–7.
[31] Krajnc A, Varlec J, Mazaj M, Ristic A, Logar NZ, Mali G. Superior performance of microporous aluminophosphate with LTA topology in solar-energy storage and heat reallocation. Adv Energy Mater 2017;7(11):1601815.
[32] LaPotin A, Kim H, Rao SR, Wang EN. Adsorption-based atmospheric water harvesting: impact of material and component properties on system-level performance. Acc Chem Res 2019;52(6):1588–97.
[33] Myat A, Kim Choon N, Thu K, Kim YD. Experimental investigation on the optimal performance of Zeolite-water adsorption chiller. Appl Energy 2013;102:582–90.
[34] de Lange MF, Verouden KJFM, Vlugt TJH, Gascon J, Kapteijn F. Adsorption-driven heat pumps: the potential of metal–organic frameworks. Chem Rev 2015;115(22):12205–50.
[35] Oppenheim JJ, Ho CH, Alezi D, Andrews JL, Chen TY, Dinakar B, et al. Cooperative interactions with water drive hysteresis in a hydrophilic metal–organic framework. Chem Mater 2024;36(7):3395–404.
[36] Hanikel N, Prevot MS, Yaghi OM. MOF water harvesters. Nat Nanotechnol 2020;15(5):348–55.
[37] Alvarez E, Guillou N, Martineau C, Bueken B, Van de Voorde B, Le Guillouzer C, et al. The structure of the aluminum fumarate metal–organic framework A520. Angew Chem Int Ed 2015;54(12):3664–8.
[38] Jeremias F, Fröhlich D, Janiak C, Henninger SK. Advancement of sorption-based heat transformation by a metal coating of highly-stable, hydrophilic aluminium fumarate MOF. RSC Adv 2014;4(46):24073–82.
[39] Lenzen D, Zhao J, Ernst SJ, Wahiduzzaman M, Ken Inge A, Fröhlich D, et al. A metal–organic framework for efficient water-based ultra-low-temperature-driven cooling. Nat Commun 2019;10(1):3025.
[40] Furukawa H, Gandara F, Zhang YB, Jiang J, Queen WL, Hudson MR, et al. Water adsorption in porous metal–organic frameworks and related materials. J Am Chem Soc 2014;136(11):4369–81.
[41] Cho KH, Mileo PGM, Lee JS, Lee UH, Park J, Cho SJ, et al. Defective Zr-fumarate MOFs enable high-efficiency adsorption heat allocations. ACS Appl Mater Interfaces 2021;13(1):1723–34.
[42] Lee JS, Yoon JW, Mileo PGM, Cho KH, Park J, Kim K, et al. Porous metal–organic framework CUK-1 for adsorption heat allocation toward green applications of natural refrigerant water. ACS Appl Mater Interfaces 2019;11(29):25778–89.
[43] Alezi D, Oppenheim JJ, Sarver PJ, Iliescu A, Dinakar B, Dinca M. Tunable low-relative humidity and high-capacity water adsorption in a bibenzotriazole metal–organic framework. J Am Chem Soc 2023;145(46):25233–41.

[44] Wright AM, Rieth AJ, Yang S, Wang EN, Dinca M. Precise control of pore hydrophilicity enabled by post-synthetic cation exchange in metal–organic frameworks. Chem Sci 2018;9(15):3856–9.
[45] Rieth AJ, Wright AM, Skorupskii G, Mancuso JL, Hendon CH, Dinca M. Record-setting sorbents for reversible water uptake by systematic anion exchanges in metal–organic frameworks. J Am Chem Soc 2019;141(35):13858–66.
[46] Rieth AJ, Yang S, Wang EN, Dinca M. Record atmospheric fresh water capture and heat transfer with a material operating at the water uptake reversibility limit. ACS Cent Sci 2017;3(6):668–72.
[47] Bagi S, Wright AM, Oppenheim J, Dinca M, Roman-Leshkov Y. Accelerated synthesis of a Ni_2Cl_2(BTDD) metal–organic framework in a continuous flow reactor for atmospheric water capture. ACS Sustain Chem Eng 2021;9(11):3996–4003.
[48] Wang S, Lee JS, Wahiduzzaman M, Park J, Muschi M, Martineau-Corcos C, et al. A robust large-pore zirconium carboxylate metal–organic framework for energy-efficient water-sorption-driven refrigeration. Nat Energy 2018;3(11):985–93.
[49] Li B, Lu FF, Gu XW, Shao K, Wu E, Qian G. Immobilization of Lewis basic nitrogen sites into a chemically stable metal–organic framework for benchmark water-sorption-driven heat allocations. Adv Sci 2022;9(11):e2105556.
[50] Canivet J, Bonnefoy J, Daniel C, Legrand A, Coasne B, Farrusseng D. Structure-property relationships of water adsorption in metal–organic frameworks. New J Chem 2014;38(7):3102–11.
[51] Alawadhi AH, Chheda S, Stroscio GD, Rong ZC, Kurandina D, Nguyen HL, et al. Harvesting water from air with high-capacity, stable furan-based metal–organic frameworks. J Am Chem Soc 2024;146(3):2160–6.
[52] Reinsch H, van der Veen MA, Gil B, Marszalek B, Verbiest T, de Vos D, et al. Structures, sorption characteristics, and nonlinear optical properties of a new series of highly stable aluminum MOFs. Chem Mater 2013;25(1):17–26.
[53] Matemb Ma Ntep TJ, Wahiduzzaman M, Laurenz E, Cornu I, Mouchaham G, Dovgaliuk I, et al. When polymorphism in metal–organic frameworks enables water sorption profile tunability for enhancing heat allocation and water harvesting performance. Adv Mater 2024;36(12):2211302.
[54] Cadiau A, Lee JS, Damasceno Borges D, Fabry P, Devic T, Wharmby MT, et al. Design of hydrophilic metal organic framework water adsorbents for heat reallocation. Adv Mater 2015;27(32):4775–80.
[55] Cho KH, Borges DD, Lee UH, Lee JS, Yoon JW, Cho SJ, et al. Rational design of a robust aluminum metal-organic framework for multi-purpose water-sorption-driven heat allocations. Nat Commun 2020;11(1):5112.
[56] Oppenheim JJ, Dinca M. Isoreticular curves: a theory of capillary condensation to model water sorption within microporous sorbents. J Am Chem Soc 2024;146(30):20615–26.
[57] Gaab M, Trukhan N, Maurer S, Gummaraju R, Müller U. The progression of Al-based metal-organic frameworks-from academic research to industrial production and applications. Microporous Mesoporous Mater 2012;157:131–6.
[58] Zhang Q, Dong S, Shao P, Zhu Y, Mu Z, Sheng D, et al. Covalent organic framework-based porous ionomers for high-performance fuel cells. Science 2022;378(6616):181–6.
[59] Li HF, Li HY, Dai QQ, Li H, Brédas JL. Hydrolytic stability of boronate ester-linked covalent organic frameworks. Adv Theory Simul 2018;1(2):1700015.
[60] Kandambeth S, Dey K, Banerjee R. Covalent organic frameworks: chemistry beyond the structure. J Am Chem Soc 2019;141(5):1807–22.
[61] Nguyen HL, Hanikel N, Lyle SJ, Zhu C, Proserpio DM, Yaghi OM. A porous covalent organic framework with voided square grid topology for atmospheric water harvesting. J Am Chem Soc 2020;142(5):2218–21.
[62] Biswal BP, Kandambeth S, Chandra S, Shinde DB, Bera S, Karak S, et al. Pore surface engineering in porous, chemically stable covalent organic frameworks for water adsorption. J Mater Chem A Mater Energy Sustain 2015;3(47):23664–9.
[63] Li J, Jing XC, Li QQ, Li SW, Gao X, Feng X, et al. Bulk COFs and COF nanosheets for electrochemical energy storage and conversion. Chem Soc Rev 2020;49(11):3565–604.
[64] Zhao S, Jiang C, Fan J, Hong S, Mei P, Yao R, et al. Hydrophilicity gradient in covalent organic frameworks for membrane distillation. Nat Mater 2021;20(11):1551–8.
[65] Zhu Q, Wang X, Clowes R, Cui P, Chen LJ, Little MA, et al. 3D cage COFs: a dynamic three-dimensional covalent organic framework with high-connectivity organic cage nodes. J Am Chem Soc 2020;142(39):16842–8.
[66] Ma J, Fu XB, Li Y, Xia T, Pan L, Yao YF. Solid-state NMR study of adsorbed water molecules in covalent organic framework materials. Microporous Mesoporous Mater 2020;305:110287.
[67] Stegbauer L, Hahn MW, Jentys A, Savasci G, Ochsenfeld C, Lercher JA, et al. Tunable water and CO_2 sorption properties in isostructural azine-based covalent organic frameworks through polarity engineering. Chem Mater 2015;27(23):7874–81.
[68] Fritz PW, Coskun A. Postfunctionalized covalent organic frameworks for water harvesting. ACS Cent Sci 2022;8(7):871–3.
[69] Nguyen HL, Gropp C, Hanikel N, Möckel A, Lund A, Yaghi OM. Hydrazine-hydrazide-linked covalent organic frameworks for water harvesting. ACS Cent Sci 2022;8(7):926–32.
[70] Nguyen HL. Covalent organic frameworks for atmospheric water harvesting. Adv Mater 2023;35(17):2300018.
[71] Tan KT, Tao SS, Huang N, Jiang DL. Water cluster in hydrophobic crystalline porous covalent organic frameworks. Nat Commun 2021;12(1):6747.
[72] Chen LH, Han WK, Yan XD, Zhang JW, Jiang YQ, Gu ZG. A highly stable ortho-ketoenamine covalent organic framework with balanced hydrophilic and hydrophobic sites for atmospheric water harvesting. ChemSusChem 2022;15(24):e202201824.
[73] Lin RB, He Y, Li P, Wang H, Zhou W, Chen B. Multifunctional porous hydrogen-bonded organic framework materials. Chem Soc Rev 2019;48(5):1362–89.
[74] Lee WG, Yoon TU, Bae YS, Kim KS, Baek SB. Selective separation of Xe/Kr and adsorption of water in a microporous hydrogen-bonded organic framework. RSC Adv 2019;9(63):36808–14.
[75] Yang Q, Wang Y, Shang Y, Du J, Yin J, Liu D, et al. Three hydrogen-bonded organic frameworks with water-induced single-crystal-to-single-crystal transformation and high proton conductivity. Cryst Growth Des 2020;20(5):3456–65.
[76] Roques N, Mouchaham G, Duhayon C, Brandes S, Tachon A, Weber G, et al. A robust nanoporous supramolecular metal–organic framework based on ionic hydrogen bonds. Chemistry 2014;20(37):11690–4.
[77] Luo YH, He XT, Hong DL, Chen C, Chen FH, Jiao J, et al. A dynamic 3D hydrogen-bonded organic frameworks with highly water affinity. Adv Funct Mater 2018;28(48):1804822.
[78] Boer SA, Conte L, Tarzia A, Huxley MT, Gardiner MG, Appadoo DRT, et al. Water sorption controls extreme single-crystal-to-single-crystal molecular reorganization in hydrogen bonded organic frameworks. Chemistry 2022;28(57):e202201929.
[79] Ma K, Li P, Xin JH, Chen Y, Chen Z, Goswami S, et al. Ultrastable mesoporous hydrogen-bonded organic framework-based fiber composites toward mustard gas detoxification. Cell Rep Phys Sci 2020;1(2):100024.
[80] Roques N, Tovar-Molle A, Duhayon C, Brandes S, Spiess A, Janiak C, et al. Modulation of the sorption characteristics for an H-bonded porous architecture by varying the chemical functionalization of the channel walls. Chemistry 2022;28(61):e202201935.
[81] Liu ZL, Xu JX, Xu M, Huang CF, Wang RZ, Li TX, et al. Ultralow-temperature-driven water-based sorption refrigeration enabled by low-cost zeolite-like porous aluminophosphate. Nat Commun 2022;13(1):193.
[82] Kim YD, Thu K, Ng KC. Adsorption characteristics of water vapor on ferroaluminophosphate for desalination cycle. Desalination 2014;344:350–6.
[83] de Lange MF, Zeng T, Vlugt TJH, Gascon J, Kapteijn F. Manufacture of dense CAU-10-H coatings for application in adsorption driven heat pumps: optimization and characterization. CrystEngComm 2015;17(31):5911–20.
[84] Yoon TU, Baek SB, Kim D, Kim EJ, Lee WG, Singh BK, et al. Efficient separation of C_2 hydrocarbons in a permanently porous hydrogen-bonded organic framework. Chem Commun 2018;54(67):9360–3.
[85] Li J, Wang Y, Chen Y, Xiong Q, Yang J, Li L, et al. Round-the-clock water harvesting from dry air using a metal–organic framework. Chin J Chem Eng 2022;49:170–7.
[86] Cao HH, Shi L, Xiong ZY, Zhu HY, Wang H, Wang K, et al. Two-periodic MoS_2-type metal–organic frameworks with intrinsic intralayer porosity for high-capacity water sorption. Adv Mater 2025;37(4):2414362.
[87] Severino MI, Gkaniatsou E, Nouar F, Pinto ML, Serre C. MOFs industrialization: a complete assessment of production costs. Faraday Discuss 2021;231:326–41.
[88] Zheng ZL, Nguyen HL, Hanikel N, Li KKY, Zhou ZH, Ma TQ, et al. High-yield, green and scalable methods for producing MOF-303 for water harvesting from desert air. Nat Protoc 2023;18(1):136–56.
[89] Zheng Z, Alawadhi AH, Yaghi OM. Green synthesis and scale-up of MOFs for water harvesting from air. Mol Front J 2023;7(01n02):20–39.
[90] Li TX, Wu MQ, Xu JX, Du RX, Yan TS, Wang PF, et al. Simultaneous atmospheric water production and 24-hour power generation enabled by moisture-induced energy harvesting. Nat Commun 2022;13(1):6771.
[91] Song W, Zheng Z, Alawadhi AH, Yaghi OM. MOF water harvester produces water from Death Valley desert air in ambient sunlight. Nat Water 2023;1(7):626–34.
[92] Tao Y, Li Q, Wu Q, Li H. Embedding metal foam into metal–organic framework monoliths for triggering a highly efficient release of adsorbed atmospheric water by localized eddy current heating. Mater Horiz 2021;8(5):1439–45.
[93] Li Q, Ying Y, Tao Y, Li H. Assemblable carbon fiber/metal–organic framework monoliths for energy-efficient atmospheric water harvesting. Ind Eng Chem Res 2022;61(3):1344–54.
[94] Wu QN, Su W, Li QQ, Tao YL, Li HQ. Enabling continuous and improved solar-driven atmospheric water harvesting with Ti_3C_2-incorporated metal–organic framework monoliths. ACS Appl Mater Interfaces 2021;13(32):38906–15.
[95] Bai ZY, Wang PF, Xu JX, Wang RZ, Li TX. Progress and perspectives of sorption-based atmospheric water harvesting for sustainable water generation: materials, devices, and systems. Sci Bull 2024;69(5):671–87.
[96] Feng YH, Wang RZ, Ge TS. Pathways to energy-efficient water production from the atmosphere. Adv Sci 2022;9(36):2204508.
[97] Bezrukov AA, O'Hearn DJ, Gascon-Perez V, Darwish S, Kumar A, Sanda S, et al. Metal–organic frameworks as regeneration optimized sorbents for atmospheric water harvesting. Cell Rep Phys Sci 2023;4(2):101252.
[98] Almassad HA, Abaza RI, Siwwan L, Al-Maythalony B, Cordova KE. Environmentally adaptive MOF-based device enables continuous self-optimizing atmospheric water harvesting. Nat Commun 2022;13(1):4873.
[99] Wright AM, Kapelewski MT, Marx S, Farha OK, Morris W. Transitioning metal–organic frameworks from the laboratory to market through applied research. Nat Mater 2025;24(2):178–87.

[100] Farrusseng D, Daniel C, Hamill C, Casaban J, Didriksen T, Blom R, et al. Adsorber heat exchanger using Al-fumarate beads for heat-pump applications—a transport study. Faraday Discuss 2021;225:384–402.
[101] Chen Z, Shao Z, Tang Y, Deng F, Du S, Wang R. Study of the scale-up effect on the water sorption performance of MOF materials. ACS Mater Au 2023;3(1):43–54.
[102] Fuchs A, Knechtel F, Wang HZ, Ji Z, Wuttke S, Yaghi OM, et al. Water harvesting at the single-crystal level. J Am Chem Soc 2023;145(26):14324–34.
[103] Terzis A, Ramachandran A, Wang KC, Asheghi M, Goodson KE, Santiago JG. High-frequency water vapor sorption cycling using fluidization of metal–organic frameworks. Cell Rep Phys Sci 2020;1(5):100057.
[104] European Commission. Technology readiness levels (TRL). In: Horizon 2020 work programme 2014–2015. Brussels: European Commission; 2014.
[105] Source global. Own your source of drinking water [Internet]. Scottsdale: Source global; undated [cited 2025 Sep 6]. Available from: https://www.source.co/.
[106] Wei Z, Wang J, Guo S, Tan SC. Towards highly salt-rejecting solar interfacial evaporation: photothermal materials selection, structural designs, and energy management. Nano Res Energy 2022;1:9120014.
[107] Ahmad S, Siddiqui AR, Yang KJ, Zhou M, Ali HM, Hardian R, et al. Lubricated surface in a vertical double-sided architecture for radiative cooling and atmospheric water harvesting. Adv Mater 2024;36(51):2404037.
[108] Zhou M, Song HM, Xu XY, Shahsafi A, Qu YR, Xia ZY, et al. Vapor condensation with daytime radiative cooling. Proc Natl Acad Sci USA 2021;118(14):e2019292118.
[109] Xu ZX, Wang YM, Lin LC. Connectivity analysis of adsorption sites in metal–organic frameworks for facilitated water adsorption. ACS Appl Mater Interfaces 2023;15(40):47081–93.
[110] Datar A, Witman M, Lin LC. Improving computational assessment of porous materials for water adsorption applications via flat histogram methods. J Phys Chem C 2021;125(7):4253–66.
[111] Datar A, Witman M, Lin LC. Monte Carlo simulations for water adsorption in porous materials: best practices and new insights. AIChE J 2021;67(12):e17447.
[112] Wang YM, Datar A, Xu ZX, Lin LC. In silico screening of metal–organic frameworks for water harvesting. J Phys Chem C 2024;128(1):384–95.
[113] Liu Z, Shen D, Cai S, Tu Z, Li S. Machine learning-assisted prediction of water adsorption isotherms and cooling performance. J Mater Chem A Mater Energy Sustain 2023;11(36):19455–64.
[114] Han B, Chakraborty A. Machine learning optimized adsorption heat transformations from adsorbents screening to enhanced performances. Energy Convers Manage 2025;344:120272.
[115] Zheng ZL, Alawadhi AH, Chheda S, Neumann SE, Rampal N, Liu SC, et al. Shaping the water-harvesting behavior of metal–organic frameworks aided by fine-tuned GPT models. J Am Chem Soc 2023;145(51):28284–95.
[116] Guo S, Zhang YX, Tan SC. Device design and optimization of sorption-based atmospheric water harvesters. Device 2023;1(4):100099.
[117] Zhao G, Moulijn JA, Kapteijn F, Dautzenberg FM, Xu B, Lu Y. Monolithic fiber/foam-structured catalysts: beyond honeycombs and micro-channels. Catal Rev 2023;66(5):1870–950.
[118] Kapteijn F, Moulijn JA. Structured catalysts and reactors—perspectives for demanding applications. Catal Today 2022;383:5–14.
[119] Gascon J, van Ommen JR, Moulijn JA, Kapteijn F. Structuring catalyst and reactor—an inviting avenue to process intensification. Catal Sci Technol 2015;5(2):807–17.
[120] Zhang YX, Tan SC. Best practices for solar water production technologies. Nat Sustain 2022;5(7):554–6.
[121] Yang KJ, Pan TT, Ferhat N, Felix AI, Waller RE, Hong PY, et al. A solar-driven atmospheric water extractor for off-grid freshwater generation and irrigation. Nat Commun 2024;15(1):6260.
[122] Guo S, Tan SC. Unlocking solar-driven synergistic clean water harvesting and sustainable fuel production. Joule 2024;8(2):291–4.